

# Missing bits of the solar jigsaw puzzle: small-scale, kinetic effects in coronal studies

David Tsiklauri

*Joule Physics Laboratory, Newton Building, University of Salford, Greater Manchester, M5 4WT, UK*

Accepted xxxx December xxx. Received xxxx December xx; in original form xxxx October xx

## ABSTRACT

The solar corona, anomalously hot outer atmosphere of the Sun, is traditionally described by magnetohydrodynamic, fluid-like approach. Here we review some recent developments when, instead, a full kinetic description is used. It is shown that some of the main unsolved problems of solar physics, such as coronal heating and solar flare particle acceleration can be viewed in a new light when the small-scale, kinetic plasma description methods are used.

## 1 INTRODUCTION

Solar corona, a tenuous and very hot outer part of the solar atmosphere which sits on top of other layers (photosphere, chromosphere, and the transition region) can be seen either in white light observations during the solar eclipses (because of  $10^6$  times more flux of visible photospheric photons is otherwise outshining it) or in extreme ultra-violet and X-ray observations from space (because of atmospheric absorption of the short wavelength radiation). Campbell & Moore (1919) describe the first successful observations of the green coronal line  $\lambda = 5303\text{\AA}$  by W. Harkness and independently by C.A. Young during the total solar eclipse of August 7, 1869. This "new" line was attributed to a new chemical element "coronium". It was easy to make such a mistake because just a year before, 1868, during the solar eclipse Frankland & Lockyer (1868) discovered a prominent yellow line  $\lambda = 5880\text{\AA}$ , which could not be ascribed to any known chemical element at the time. This marked a discovery of Helium after Greek word 'Helios' meaning 'Sun'. On Earth helium was only found about 10 years later by W. Ramsay. The blunder with coronium went on for quite some time. Moreover, as described by Birkeland (1908), the new gas geo-coronium extends from 200 km above Earth into the space, and that the steady auroral arcs are due to electric luminescence in this gas. The truth had to wait until the beginning of 1940s. In his George Darwin lecture of the Royal Astronomical Society (Edlén, B. 1945) entitled "The identification of the coronal lines" Edlén describes the process of realising that the mysterious coronal lines, including the green coronal line  $\lambda = 5303\text{\AA}$ , come from so-called forbidden lines of highly ionised metals. For example, the most intense green coronal line comes from FeXIV, iron atom with 13 electrons stripped off. Edlén rightfully acknowledges that the correct identification of the coronal lines was triggered by a letter of 13 February 1937 sent to him by W. Grotrian. These forbidden lines are emitted from energetically unfavourable metastable atomic energy levels. Under normal laboratory conditions electrons do not readily make transitions from the metastable states to lower energy states (whilst emitting

photons) due collisional de-excitation. In the extremely rarefied conditions of the solar corona such transitions become possible. The highly ionised metal ions can only be created in extremely hot conditions  $T > \text{few } 10^6$  K. Thus, at the time it was rather difficult to accept that solar corona is so hot. Especially because this seemed in an apparent violation of the second law of thermodynamics (in Rudolf Clausius's formulation) that the heat cannot flow from a cold body (photosphere at  $\approx 6000$  K) to a hotter body (corona at  $\text{few } 10^6$  K). In this manner, one of the major unsolved problem in solar physics has emerged: which physical mechanisms are responsible for heating of solar corona? Some significant progress has been made, particularly, with the advent of space era in solving the coronal heating problem (see e.g. chapter 9 in Aschwanden (2006)). As it happens in science, in general, the progress has led to yet more, previously unknown challenges such as finding the answers to the questions: (i) Why solar wind speed in the polar regions is twice higher during the solar minimum than plausible solar wind models can explain? (ii) Why the solar flares, the violent events in the corona when magnetic energy is converted into other forms, occur on timescales much shorter than the plausible resistive timescales predict? (iii) Why the most of the solar flare energy is taken away by the accelerated, super-thermal particles? and so on. It is important to realise that reproducing or mimicking the reality in (mostly) numerical models does not necessarily mean that we have an *understanding* of physical mechanisms in action. Here are a few examples e.g. in simple 1D coronal loop models a steady state of  $\text{few } 10^6$  K plasma can be maintained by balancing an *ad hoc* heat input with realistic losses such as heat conduction, radiation, etc, or even time-varying flare dynamics can be simulated (Tsiklauri et al. 2004). More realistic 3D models (Gudiksen & Nordlund 2005; Gudiksen 2009) mimic the solar coronal observations and yet use unrealistically high magnetic resistivity. No wonder if one puts sufficient heating or artificially adjusts dissipation coefficients, a  $\text{few } 10^6$  K plasma can be obtained that "looks like" the solar corona. But did we learn what generates this heat or makes the dis-

sipation coefficients anomalously high? Albeit, the answer is no. Notwithstanding, something useful can be learnt e.g. where spatially heat needs to be deposited to reproduce the observations. Similarly, consider the sophisticated solar wind models which solve numerically fluid-like equations for electrons, protons and alpha particles (Li et al. 2006). Indeed, such models can reproduce twice as high solar wind speeds in the polar regions than near the solar equatorial plane, as observed during solar minima. But, this is obtained based on an *ad hoc* energy flux injected into the both ion species. Again, it comes as no surprise that *ad hoc* energy flux (essentially an additional momentum added) to the ion species produces observed fast solar wind speeds. Again, no answer is provided to the main question: what provides this additional energy flux (momentum)? Is it due to absorption of waves? or due to some microscopic reconnection events at the base of the corona? As to the question of why the most of the solar flare energy is taken away by the accelerated particles, the situation is analogous. Kinetic-scale Particle-In-Cell modelling (Tsiklauri & Haruki 2008a) can in principle reproduce the solar flare observations in that within one Alfvén time, somewhat less than half ( $\leq 40\%$ ) of the initial total (roughly magnetic) energy is converted into the kinetic energy of electrons, and somewhat more than half ( $\leq 60\%$ ) into kinetic energy of ions (similar to solar flare observations). Also, a sizable fraction (up to 20%) of the magnetic energy can be released/converted into other forms such as kinetic energy of super-thermal particles and to much small extent waves. However, such simulations are performed usually in a domain sizes of several hundreds of electron Debye length  $\lambda_D = v_{te}/\omega_{pe} = 2.2 \times 10^{-3}$  m, which is about  $10^5 - 10^6$  times smaller than the solar flare particle acceleration site. Here  $v_{te} = \sqrt{k_B T/m_e}$  is electron thermal speed taken at  $T = 10^6$  K and  $\omega_{pe} = \sqrt{ne^2/(m_e \epsilon_0)}$  is electron plasma frequency taken at  $n = 10^{15} \text{ m}^{-3}$ , commensurate to solar corona. The question is whether realistic behaviour mimicked in small simulation domains will also hold if they are up-scaled to realistic sizes? The situation is analogous to the stability of plasma in thermonuclear fusion devices such as Tokamaks: small-scale ("laboratory"-scale) versions behave quite differently from the plasma stability point of view than the large, "factory"-scale ones.

## 2 MAGNETOHYDRODYNAMIC (MHD) VS KINETIC PLASMA DESCRIPTION

The above discussion about the spatial scales,  $L$ , – the characteristic length scales of a physical system over which properties of physical quantities (e.g. magnetic field of an active region in the solar corona) change – brings us to the following dichotomy or a dilemma. One one hand, solar corona is well described by the MHD approach. This is because if we take  $L$  as the hydrostatic scale-height of the corona (height over which pressure drops  $e$ -times)  $\approx 50 \times 10^6$  m, this is much larger than all relevant kinetic scales: (i)  $c/\omega_{pi} \approx 7.2$  m, ion (proton) inertial length (also called ion skin depth), (ii)  $c/\omega_{pe} \approx 0.2$  m electron inertial length (also called electron skin depth), (iii)  $r_{L,e} = v_{te}/\omega_{ce} = 2.2 \times 10^{-3}$  m electron Larmor radius. ( $\omega_{ce} = eB/m_e$  is the electron cyclotron frequency, which quantifies rotation of electrons around the magnetic field on their helical path.) On the other hand,

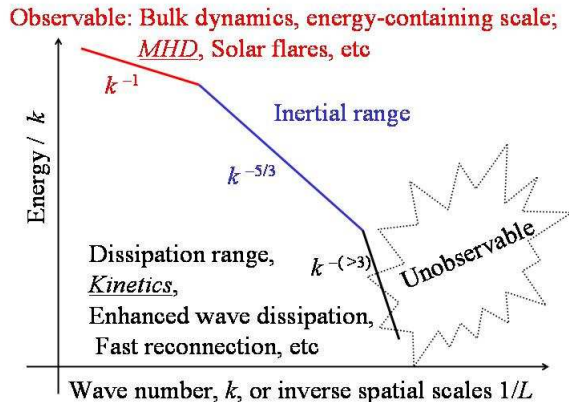


**Figure 1.** A sketch of typical power spectrum (energy per wavenumber  $k$ , (i.e.  $E/k$ ), versus  $k$ ) of magnetic fluctuations in the solar wind. Adopted from Goldstein & Roberts (1995).

all interesting physical processes such as wave dissipation, nano-scale *fast* reconnection (coronal plasma heating) and particle acceleration (during flares) occur at small, kinetic scales. The dichotomy, depicted in Fig. 1, is in that the bulk plasma dynamics in the solar corona (where most of the energy is stored) is observable remotely from Earth (typical smallest coronal structures resolved e.g. with TRACE satellite is  $0.5''$  i.e.  $\approx 0.36 \times 10^6$  m on the Sun). But the above interesting physical processes all operate at scales below 10 m. Thus, unless an in-situ probes are sent to the solar corona the kinetic-scales processes will never be observed. It seems unlikely humankind will ever come up with materials (for the probes) which will withstand the heat of the coronal environment. However, ESA has plans for Proba mission (<http://www.esa.int/esaMI/Proba/>), in which the telescope of Proba-3's solar coronagraph will be mounted on one of the spacecraft, while the other craft is manoeuvred to accurately occult (mask) the main disc of the Sun. With the proposed Proba-3 arrangement, it is anticipated that accurate measurements will be possible from 1.05 to 3.2 solar radii. Note that the discussion about spatial scales  $L$  can always be cast into temporal scales,  $T$  or frequencies  $f = 1/T$  by using characteristic speed of processes  $V_{char}$  via  $T = L/V_{char}$ . For example  $V_{char}$  can be the Alfvén speed,  $V_A = B_0/\sqrt{\mu_0 n m_i} = B_0/\sqrt{\mu_0 \rho}$ , if MHD-scale processes are considered. This would equally be applicable to waves and reconnection. In the latter case reconnection outflow speeds would be implied, while in the case of former – phase speed of the wave.

Let us briefly discuss conditions of when the above mentioned kinetic scales become important. Strictly speaking MHD equations are scale-free, in a sense that there is no physical spatial scale appearing in the equations (except  $L$  which is an *arbitrary* size of the system, which simply needs to stay macroscopic so that continuum mechanical (fluid-like) description remains valid). The devil is in the detail, however. In order to obtain closed set of equations one needs to express the electric field by means of other physical quantities. In MHD, the induction equation for the magnetic field is obtained by plugging in  $E$  into the Faraday's law (from the Maxwell's equations)  $\partial \vec{B}/\partial t = \nabla \times \vec{E}$ . Intrinsic physical

scales start appearing when instead of usual MHD-version generalised Ohm's law (Drake & Shay 2007), p. 89,

$$\vec{E} = -\vec{v} \times \vec{B} + \eta \vec{j} \quad (1)$$

one starts to use a more general form:

$$\vec{E} = -\vec{v} \times \vec{B} + \eta \vec{j} + \frac{\vec{j} \times \vec{B}}{ne} + \frac{m_e}{ne^2} \left( \frac{\partial \vec{j}}{\partial t} + \nabla \cdot \left( \vec{j} \vec{v} + \vec{v} \vec{j} - \frac{\vec{j} \vec{j}}{ne} \right) \right) - \frac{\nabla \cdot P_e}{ne} \quad (2)$$

Eq.(2) essentially can be obtained from the electron equation of motion if electron speed  $\vec{v}_e$  is replaced by  $\vec{v}_e = \vec{v}_i - \vec{j}/ne$ . The latter is mathematical statement of: when electron and ion speeds are different, this causes charge separation electric field and hence current  $\vec{j} = en(\vec{v}_i - \vec{v}_e)$ . In MHD, however, ion and electron separate dynamics is ignored and  $\vec{v}_i = \vec{v}_e = \vec{v}$ . It can be shown (Drake & Shay 2007) that each of the non-MHD terms (second line of Eq.(2)) have intrinsic spatial scales associated with them: (i) the term containing  $\vec{j} \times \vec{B}$  (called Hall term) becomes important on scales comparable to  $c/\omega_{pi}$ , ion skin depth; (ii) the term containing  $(m_e/ne^2)\partial\vec{j}/\partial t$  (called electron inertia term) becomes important on,  $c/\omega_{pe}$ , electron skin depth scale; and finally (iii) the term containing the divergence of the pressure tensor,  $\nabla \cdot P_e$ , (called pressure tensor term) becomes important on scales comparable to  $r_{L,e}$ , electron Larmor radius.

### 3 SMALL SCALE EFFECTS IN RECONNECTION

In order to better understand ordering of different spatial scales let us consider a simple problem of steady reconnection when oppositely directed magnetic field lines are brought into a diffusion region by an inflow of plasma, then they change connectivity and plasma outflow carries the field lines away. The change of connectivity occurs in the diffusion region which has width  $\delta$  and length  $\Delta$ . In MHD, in the simplest possible formulation (Sweet-Parker model): (i) Bernoulli equation determines the outflow speed being the Alfvén speed,  $V_{out} = V_A$ ; (ii) continuity equation prescribes in the reconnection inflow speed  $V_{in} = (\delta/\Delta)V_A$ ; while (iii) the generalised Ohm's law in which the advection term  $\vec{v} \times \vec{B}$  is balanced by the resistive term  $\eta \vec{j}$  sets the reconnection rate  $M_{sp} = V_{in}/V_{out} = V_{in}/V_A = S^{-1/2} \ll 1$ , where  $S \gg 1$  is the magnetic Lundquist number. Thus, in MHD Sweet-Parker model (in which  $\Delta$  is fixed at  $L$ ) is producing reconnection rates much smaller what is observed in e.g. flares in solar corona. For the parameters commensurate to solar corona ( $n = 1.0 \times 10^{15} \text{ m}^{-3}$ ,  $T = 1.0 \times 10^6 \text{ K}$ ,  $L = 10^5 \text{ m}$ ,  $B = 0.01 \text{ T}$  (100 Gauss and hence  $V_A = 6.9 \times 10^6 \text{ m s}^{-1}$ ),  $S = 3.7 \times 10^{11}$ ) the classical Sweet-Parker rate is  $M_{sp} = 1.6 \times 10^{-6}$ . The reconnection rate is also interpreted as the ratio of Alfvén time ( $\tau_A = L/V_A \approx 0.0145 \text{ s}$ ) and resistive (or reconnection) times. This means in the Sweet-Parker model resistive (or reconnection) time is  $0.0145/S^{-1/2} \text{ s} = 0.1 \text{ days}$ . On contrary, in the observations flares last for up to tens of minutes. Petschek model alleviates this problem by making the diffusion region length,  $\Delta \ll L$ . This means that the plasma inflow speed  $V_{in} = (\delta/\Delta)V_A$  a sizable fraction of the Alfvén speed making reconnection rates faster and hence flare times shorter commensurate to the

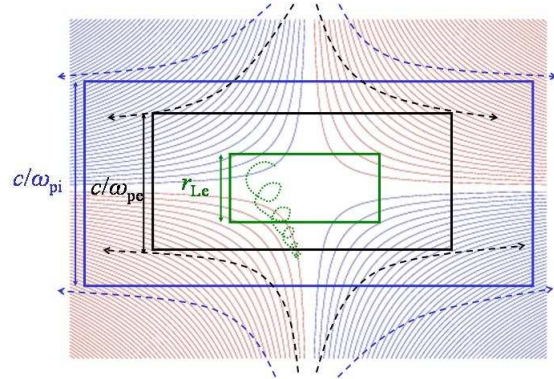


**Figure 2.** A sketch of kinetic-scale magnetic reconnection. Blue and red curves in the quadrants show an opposite sign magnetic flux. The outer, blue box shows a region where ions become demagnetised, whilst electrons are still magnetised. From this scale ( $c/\omega_{pi}$ ) and below the magnetic field is carried by electrons. Black box with width  $c/\omega_{pe}$  shows electron diffusion region where magnetic connectivity change take place. The green box with width  $r_{L,e}$  shows region where electron meandering motion makes pressure to become a tensor with off-diagonal (non-gyrotropic) terms playing a major role. Blue and black dashed lines with arrow heads show ion and electron flow, respectively. Note how ion flow deflects at the scale  $c/\omega_{pi}$ , while electron flow does so at  $c/\omega_{pe}$ . The green wiggle in the centre show an electron orbit. Its radius is small and follows a magnetic field line away from the diffusion region. The radius becomes large and motion chaotic (meandering) as the magnetic field drops to zero close to the magnetic null.

observations. However, Petschek model is a phenomenological one (not derived from the first principles) and for it to work (as demonstrated by numerous numerical simulations) it requires plasma resistivity to be non-uniform and be enhanced on the diffusion region (so-called anomalous resistivity). Whilst, the latter being quite plausible, given that turbulent transport is known to enhance the dissipation/resistive coefficients dramatically, we have not sent in-situ probes to the solar corona yet, and hence we do not know for certain whether it is turbulent or not!

It should be noted that in the laboratory plasma Magnetic reconnection experiment (MRX) measurements show indication of the reconnection rates or equivalently anomalous resistivity values 10s and even 100 times larger that Sweet-Parker model predicts (Yamada et al. 2006). The MRX experiment plasma *is not in the turbulent state*. What is observed, however, is that the reconnection rates or equivalently anomalous resistivity values are attained when the transition from collisional (resistive MHD) to collisionless (kinetic) regime takes place.

So, is there an alternative way (i) to have fast reconnection i.e. get solar flare times right? (ii) also to demonstrate that the large proportion of flare energy goes into the accelerated particles? and (iii) not to make assumptions about the turbulent state of the corona (hence postulating the anomalous resistivity)? It turns out that plasma *kinetic* approach can provide answer "cautious yes" to all of these fundamental questions. Here is how: For the solar coronal parameters: a temperature of  $1.0 \times 10^6 \text{ K}$ , Coulomb logarithm of 18.1, the Lundquist number (using Spitzer resistivity) is

$3.7 \times 10^{11}$ . Here  $L = 10^5$  m was used. One of the reasons for going beyond resistive MHD is comparing typical width of a Sweet-Parker current sheet  $\delta_{sp} = S^{-1/2}L = 0.16$  m to the ion skin depth. Typical scale associated with the Hall term in the generalised Ohm's law at which deviation from electron-ion coupled dynamics is observed is,  $c/\omega_{pi} = 7.2$  m. Here particle number density of  $n = 1.0 \times 10^{15} \text{ m}^{-3}$  has been used. Hence, the fact that  $c/(\omega_{pi}\delta_{sp}) = 44 \gg 1$  justifies going *beyond single fluid resistive MHD approximation* (a similar conclusion is reached by Yamada et al. (2006) in their Fig. 12). In other words, ion skin depth scale is reached first before resistive MHD Sweet-Parker current sheet. Let us put this fact (that  $c/(\omega_{pi}\delta_{sp}) \gg 1$ ) in the visual context using Fig. 2: On a global (bulk MHD) scale  $L$  electrons and ions in-flow towards the diffusion region (where magnetic field connectivity changes) in a coordinated way as if they are glued to each other. When the flow approaches ion skin depth scale  $c/\omega_{pi}$  ions become demagnetised (magnetic field is no longer is frozen into ion fluid) and magnetic field is carried forward by electrons. At  $c/\omega_{pi}$  scale the Hall term in the generalised Ohm's law dominates. This picture is broadly corroborated by kinetic, particle-in-cell simulations of x-point collapse (Tsiklauri & Haruki 2007). In panel (a) of Fig.3 we see that for electrons the diffusion region width is indeed  $c/\omega_{pe}$ , while for ions, panel (b) of Fig.3, the width of the region where ions start to deflect from the current sheet (region where ions become demagnetised) is about  $c/\omega_{pi} = 10c/\omega_{pe}$  (note that here the ion to electron mass ratio of  $m_i/m_e = 100$  has been used). This continues until electron skin depth scale  $c/\omega_{pe}$  is reached where electron inertia term takes over. Further down the spatial scales, when electron Larmor radius scale  $r_{L,e}$  is reached electron meandering motion (dashed green wiggled curve in Fig.2) sets in (Horiuchi & Sato 1997). This makes the non-gyrotropic (off-diagonal) components of the electron pressure tensor to dominate other terms in the generalised Ohm's law, and hence makes them responsible for breaking the frozen-in condition. The concept of pressure tensor is somewhat counter-intuitive. This can be comprehended as follows: away from the electron diffusion region pressure is scalar (isotropic) and electrons flow along (are frozen into) the magnetic field lines. Inside the the diffusion region  $\leq r_{L,e}$  electrons become demagnetised and execute meandering (rather chaotic) motions. These are such that pressure becomes different as one travels in different directions (i.e. pressure becomes a tensor as opposed to a scalar). Previous results on collisionless reconnection both in tearing unstable Harris current sheet (Kuznetsova et al. 1998; Hesse et al. 1999; Birn et al. 2001; Pritchett 2001) and stressed X-point collapse (Tsiklauri & Haruki 2007, 2008a) have shown that magnetic field is frozen into electron fluid and the term in the generalised Ohm's law that is responsible for breaking the frozen-in condition is electron pressure tensor off-diagonal (non-gyrotropic) component gradients. Thus, there is a case for inclusion of the *electron pressure tensor non-gyrotropic components* in a model of collisionless reconnection. Analytically, this was achieved by (Tsiklauri 2008). In this simple model instead of balancing the advection term in the generalised Ohm's law with the resistive term (as discussed above), non-gyrotropic components of the electron pressure tensor gradient were used. This produced simple analytical results which explain well (i) the recon-

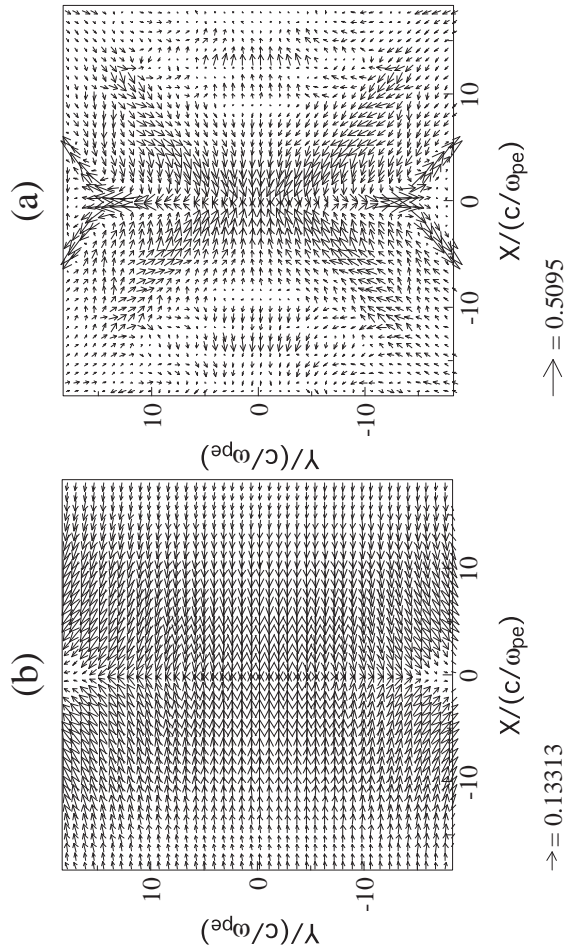


**Figure 3.** Electron (a) and ion (b) flow patterns at the peak of time-transient reconnection of x-point collapse. Adapted from Tsiklauri & Haruki (2007), who used particle-in-cell, kinetic approach for the numerical simulation. The arrow size represents instantaneous, cell-averaged velocities normalised by speed of light. Note that for electrons the diffusion region width is about  $c/\omega_{pe}$ , while ion flow deflects from the diffusion region at a width  $c/\omega_{pi}$  (here  $c/\omega_{pi} = 10c/\omega_{pe}$ ), as sketched in Fig. 2.

nection rate and (ii) width of the electron diffusion region measurements in MRX experiment.

There is a growing amount of work (Drake & Shay 2007; Tsiklauri & Haruki 2007, 2008a) that suggests that in the collisionless regime, on the scales less than  $c/\omega_{pi}$  magnetic field is frozen into the electron fluid rather than bulk of plasma. One can write in general  $\vec{v}_e = \vec{v}_i - \vec{j}/(en)$ . This relation clearly shows that in collisional regime (when the number density  $n$  is large), the difference between electron and ions speeds diminishes  $v_e = v_i = v$ . However, as one enters collisionless regime (when the number density  $n$  is small) the deviation between electron and ion speeds starts to show. In Tsiklauri & Haruki (2008a) we proposed a possible explanation why the reconnection is fast when the Hall term is included. Inclusion of the latter means that in the reconnection inflow magnetic field is frozen into *electron* fluid. As it was previously shown in Tsiklauri & Haruki (2007) (see their Figs.(7) and (11)) speed of electrons, during the reconnection peak time, is at least 4-5 times greater than that of ions. This means that electrons can bring in / take

out the magnetic field attached to them into / away from the diffusion region much faster than in the case of single fluid MHD which does not distinguish between electron-ion dynamics. Thus, it is clear that inclusion *magnetic field transport by electrons* is crucial in resolving of above mentioned problems MHD description of the solar corona faces.

To summarise, some of the time-dependent collisionless reconnection models such as tearing unstable Harris current sheet (Kuznetsova et al. 1998; Hesse et al. 1999; Birn et al. 2001; Pritchett 2001) and stressed X-point collapse (Tsiklauri & Haruki 2007, 2008a) where able: (i) to show that a sizable fraction of the magnetic energy can be converted/released into heat and accelerated, super-thermal particle energy (see e.g. Fig.13 from Tsiklauri & Haruki (2007)); (ii) obtain fast reconnection rates and hence magnetic energy release rate commensurate to solar flare observations (see e.g. Figs.3 and 9 from Tsiklauri & Haruki (2007)); (iii) reproduce the observational fact that the large proportion of flare energy goes into the accelerated particles in the correct partition, i.e. somewhat less than half (40%) of the initial total (roughly magnetic) energy is converted into the kinetic energy of electrons, and somewhat more than half (60%) into kinetic energy of ions (see e.g. Figs.3 and 4 from Tsiklauri & Haruki (2008a)); (iv) not to invoke anomalous resistivity. However, despite this success there are main challenges ahead: (i) the processes described by the collisionless reconnection models are small scale ( $< c/\omega_{pi} \approx 10$  m). Indeed, on scale less than ion skin depth magnetic field is advected into the diffusion region by electrons and since electrons are lighter and move faster, the reconnection is accordingly fast. But, sufficiently far away from the electron diffusion region, electron flow must slow down to bulk plasma speeds when MHD description takes over (ions and electrons become glued to each other), where and how this happens? Recent PIC simulations Daughton et al. (2006); Shay et al. (2007) suggest that the electron diffusion region length can extend for much longer distances downstream than previously thought. Why does this happen is not understood. (ii) How this small-scale dynamics on the kinetic scale translate into MHD scales? i.e. despite producing fast reconnection rates, these processes happen in physically small volumes. Will they affect MHD-scale (say a  $L = 10^6$  m) processes? It will be impossible to find out until we can perform a numerical simulation  $10^6\text{m} \times 10^6\text{m} \times 10^6\text{m}$  using realistic coronal active region fields as an input for Particle-In-Cell or Vlasov simulation. The latter would seem many decades away even if Moore's law (that the number of transistors that can be placed inexpensively on an integrated circuit has increased exponentially, doubling approximately every two years) continues to hold in the future. Until such times, we can do  $10\text{m} \times 10\text{m} \times 10\text{m}$  kinetic simulation and hope for the best that our models will scale correctly towards the larger (physically meaningful) spatial scales.

#### 4 SMALL SCALE EFFECTS IN WAVES

Study of MHD waves in the solar corona has seen steady progress over last two decades. There are two aspects to the study: (i) waves carry information about the medium they propagate in. This is used in the field of solar coronal seismology to infer physical parameters of the corona

(see for reviews Nakariakov & Verwichte (2005); De Moortel (2009)). For example traditional method of measuring magnetic field in solar photosphere is based on the Zeeman effect. However, in solar corona plasma is too dilute rendering this method unusable. Based on the seminal theoretical work of Edwin & Roberts (1983), transverse oscillations of solar coronal EUV loops were used to successfully measure the magnetic field (Nakariakov & Ofman 2001). (ii) waves transport mechanical (and magnetic) energy and if dissipated may produce plasma heating.

In the MHD approximation, in a uniform plasma penetrated by a uniform magnetic field,  $\vec{B}_0$ , there are three distinct types of waves: fast and slow magnetosonic and Alfvén waves.

Fast magnetosonic waves are compressible MHD waves which have an advantage of propagating across the magnetic field. This implies that the heat produced by the wave dissipation can spread across and cover a large area. The fast magnetosonic waves that are generated in the solar interior cannot reach the corona because of the reflection on the pressure/density gradient (due to gravitational stratification). Thus, initially they were excluded from coronal heating models. However, in the transversely inhomogeneous plasma there are two possibilities to couple Alfvén waves (which have no problem of crossing the gradient) with fast magnetosonic waves: either by non-linear coupling in 2.5 MHD approximation (Nakariakov et al. 1997; Tsiklauri et al. 2001); or linear (much more efficient) coupling in 3D MHD approximation (Tsiklauri & Nakariakov 2002; Tsiklauri et al. 2003).

Slow magnetosonic waves are also compressible, but propagate preferentially along the magnetic field. Normally, these waves are discounted from coronal heating candidate list on the grounds of not carrying (less by four orders of magnitude) sufficient flux De Moortel (2009). However, the latter estimate is based on the assumption of just a single harmonic (fixed frequency) and Tsiklauri & Nakariakov (2001) have demonstrated that if a wide spectrum (continuous spectrum with a plausible frequency (or wavenumber) range) of slow magnetosonic waves exists in the corona, than their dissipation would provide sufficient heating. Whether such spectrum exists is an open question. However since in the nature there is always a cascade of energy from large scales to small scales (see e.g. Fig. 1), this wide spectrum conjecture seems plausible.

Alfvén wave is an incompressible, transverse wave (such as e.g. electromagnetic wave), with frequency,  $\omega_A$ , much smaller than ion cyclotron frequency,  $\omega_{ci} = eB/m_i$ . In an Alfvén wave the background magnetic field tension provides restoring force, while plasma ions provide inertia (the two key ingredients for any oscillatory motion). Alfvén waves are easy to excite, e.g. a sheared plasma flow across magnetic field. However, they are notoriously difficult to dissipate because of small resistivity of the solar corona. i.e. Alfvén wave is a good vehicle for transporting energy (e.g. from convective motions below the photosphere into the corona), but this "vehicle" has virtually no breaks (hence cannot be stopped!). Thus, in order to deposit energy in the first  $\approx 50 \times 10^6$  m of the corona (the hydrostatic scale-height) above the transition region, some enhanced dissipation mechanisms were proposed in the past. In the solar corona, basic magnetic structure that is encountered is ei-

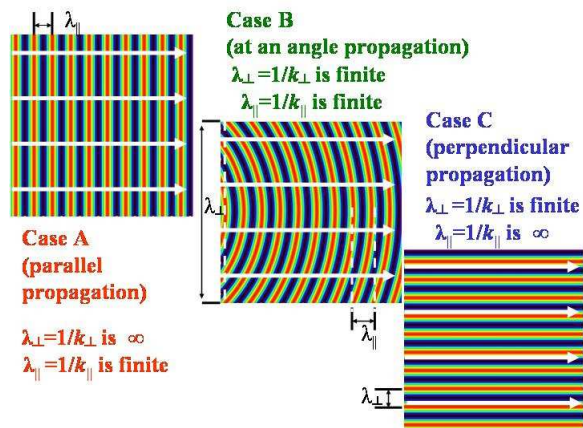


**Figure 4.** A sketch of parallel, at an angle and perpendicular propagation of a wave.

ther a closed loop (during 11-year cycle minimum more of these are found near solar equator and low latitudes); or open magnetic strictures such a plumes (during the solar minimum these are mostly located near the north and south polar regions). The common feature of these coronal structures is the density variation *across* the magnetic field. i.e. inside the loops and plumes density is enhanced by 3 – 10 times compared to the surrounding plasma. In the case of closed magnetic structures this enhanced density is believed to be due to material evaporation from denser layers of the sun such as transition region and chromosphere. In the open magnetic structures the density enhancement is either due to a solar wind and again material evaporation from below (which could be either due to reconnection or any other process which increases plasma temperature so that the balance no longer holds). There are two mechanisms for the above mentioned enhanced Alfvén wave dissipation and absorption in the solar corona: phase mixing (Heyvaerts & Priest 1983) and resonant absorption Ionson (1978). In both mechanisms transverse inhomogeneity of plasma (i.e. plasma with density variation across the uniform magnetic field) plays a crucial role (albeit for different reasons). Brief review of both topics can be found in De Moortel et al. (2008).

For particle acceleration and efficient *non-resonant* wave-particle interactions (e.g. converting wave energy to particle kinetic energy and heat if inter-particle collisions are efficient), it is necessary for a wave in question to have magnetic field-aligned electric field. The word non-resonant is crucial here because, interaction of waves with particles when (i) the wave phase speed  $V_{ph} = \omega/k$  coincides with particle (thermal) speed  $v_{th,\alpha} = \sqrt{k_B T/m_\alpha}$  leads to the Landau resonance; or (ii) to the cyclotron resonance, when the rotation frequency of the electric field vector of the circularly polarised wave,  $\omega$  coincides with the particle’s cyclotron frequency,  $\omega_{c\alpha} = eB/m_\alpha$  (and when both the wave electric field vector and particle rotate in the same direction). In the both cases particle experiences almost constant electric field, which facilitates efficient wave-particle resonant interaction. Away from the resonance  $V_{ph} \gg$  or  $\ll v_{th,\alpha}$  in the case of Landau damping; or  $\omega \gg$  or  $\ll \omega_{c\alpha}$  in the case of cyclotron resonance, wave electric field oscillates too fast or too slow and has no effect on plasma particles of species  $\alpha$ . In the MHD approximation Alfvén wave

propagates strictly along the magnetic field (with some finite parallel to the magnetic field wave number  $k_{\parallel} \neq 0$ ) as shown in case A, Fig. 4. In this case the perpendicular wave number  $k_{\perp} = 0$ . For the field aligned electric field to exist  $k_{\perp} \neq 0$  condition should be true. Case C, Fig.4 also shows why the fast magnetosonic waves are believed to be efficient particle accelerators. This because they preferentially propagate across the magnetic field and hence possess finite  $k_{\perp} \neq 0$ . For Alfvénic waves  $k_{\perp} \neq 0$  (see case B, Fig. 6) only possible when kinetic-scale effects are included. In particular, it has been realised (Hasegawa & Chen 1976) that when externally applied wave frequency becomes resonant with the Alfvén frequency  $\omega_A = k_{\parallel} V_A$ , a resonance occurs and the driving wave converts into kinetic Alfvén wave (KAW) which has the finite field-aligned electric field. More generally, generation of the parallel (magnetic field-aligned) electric field occurs when the applied low-frequency ( $\omega < \omega_{ci}$ ) Alfvén wave has  $k_{\perp}$  comparable to any of the *kinetic spatial scales*. Such Alfvén waves (with  $E_{\parallel} \neq 0$ ) are called *dispersive Alfvén waves* (DAW) (Stasiewicz et al. 2000). The latter split into two classes: kinetic Alfvén waves (KAW) and inertial Alfvén waves (IAW). The distinction between the two is drawn according to the value of plasma beta, which is the ratio of thermal and magnetic pressures, i.e.  $\beta = p/(B^2/2\mu_0)$ . Plasma beta can also be related to the ratio of the sound speed and Alfvén speed squared, i.e.  $\beta = (2/\gamma)(c_s^2/V_A^2) \approx c_s^2/V_A^2$ , the ratio of specific heats  $\gamma$  in e.g. adiabatic case is 5/3. Here  $c_s = \sqrt{\gamma p/\rho}$  is the sound speed. Physically, plasma beta prescribes importance of either thermal effects or magnetic field. E.g. in solar corona  $\beta \ll 1$  meaning that magnetic fields play a dominant role in coronal plasma behaviour. In the context of dispersive Alfvén waves plasma beta prescribes which term in the generalised Ohm’s law supports parallel electric field (Stasiewicz et al. 2000). If  $\beta < m_e/m_i$ , i.e.  $v_{te}, v_{ti} < v_A$  then the dominant mechanism for generation of parallel electric field in the generalised Ohm’s law is the electron inertia and one has inertial Alfvén waves (IAW). If  $\beta > m_e/m_i$ , i.e.  $v_{te}, v_{ti} > v_A$  then the dominant mechanism for generation of parallel electric field in the generalised Ohm’s law is electron pressure gradient and one has kinetic Alfvén waves (KAW).

In the solar corona, particle acceleration e.g. during solar flares is generally believed to be occurring as a result of magnetic reconnection. For description of particle dynamics either test particle approach (Zharkova & Gordovskyy 2005; Dalla & Browning 2008) which ignores self-consistent fields or more recently kinetic, particle-in-cell simulation (Siversky & Zharkova 2009) has been used. The problem with particle acceleration during solar flares is associated with the numbers of particles involved. In the standard flare model, reconnection event occurs higher up the corona and as result 50-80 % of the flare energy is converted into accelerated particles (electrons and ions). These rush down towards denser layers of the solar atmosphere guided by coronal magnetic field structures and produce X-ray emission via bremsstrahlung. The number of detected X-ray photons can be related (via certain model assumptions) to the number of accelerated electrons. For a typical flare more than  $10^{39}$  electrons are accelerated, yielding a huge current sheet (with a volume of  $10^{28}$  cm<sup>3</sup>) that must remain stable for more than 60 seconds. This is an unlikely course of events because of the dissolution (thin-

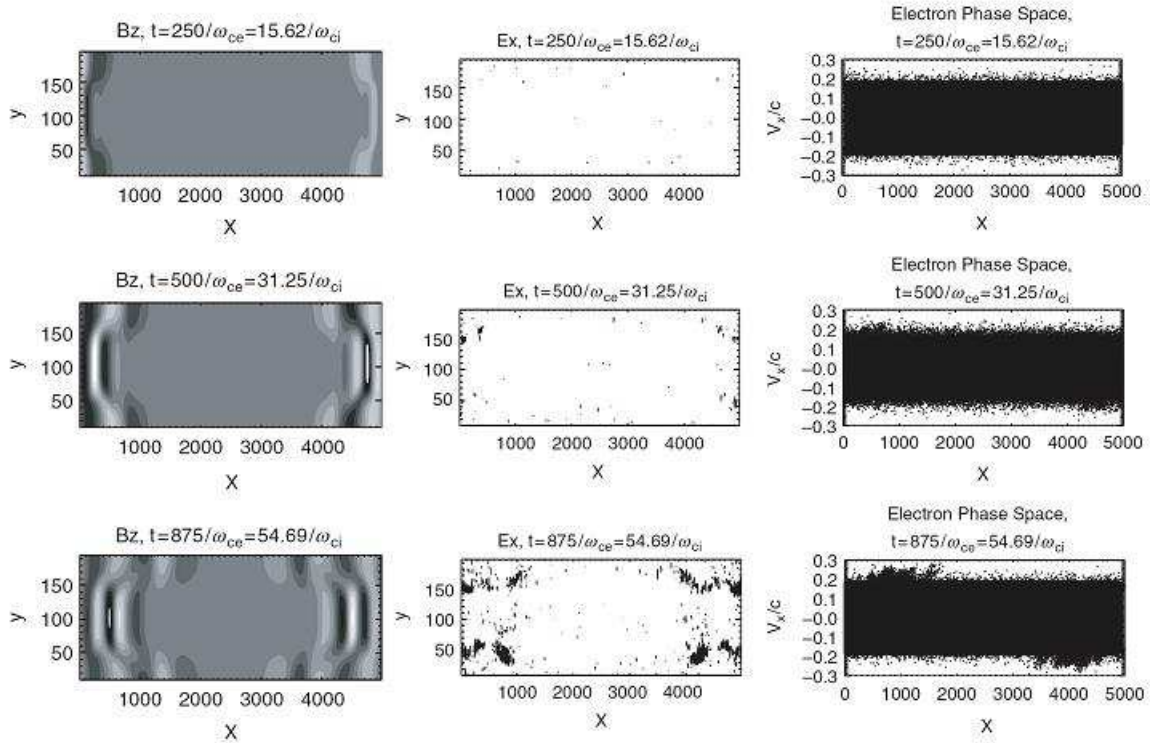


**Figure 5.** The left column shows three snapshots of Alfvén wave magnetic field component. The middle columns shows the generated parallel electric field,  $E_{\parallel}$ . The right column shows parallel velocity phase space of electrons. See text for details.

ning) of the current sheet (Brown & Melrose 1977). In effect, the above numbers imply that all of the electrons in the current sheet need to be evacuated. Another problem is with the return currents. A beam of electrons injected into plasma is known to be compensated by the generated counter beam. Thus, expecting a bunch of all  $10^{39}$  electrons happily travels towards the footpoints of the magnetic structure is naive. A viable alternative for transporting flare energy by the beam of accelerated particles, is waves. As we know waves can transport energy without mass transport. Therefore, if flare energy is delivered to footpoints by waves then the above mentioned difficulties (the number problem and return currents can be avoided). In this scenario, reconnection flare event produces dispersive Alfvén waves (which possess parallel electric fields). These subsequently travel to the footpoints, then accelerate particles in the vicinity of footpoints. The accelerated particles (mostly electrons, because these waves are known to preferentially accelerate electrons due to their small inertia, whilst producing ion heating – broadening of their distribution function), in turn, produce the observed X-rays via the bremsstrahlung. Using particle-in-cell simulation, Tsiklauri et al. (2005) have recently explored how circularly polarised Alfvén wave with  $\omega = 0.3\omega_{ci}$  propagates in a transversely inhomogeneous plasma. This frequency is somewhat higher than that for MHD wave and yet smaller than ion cyclotron resonance. Such wave strictly speaking is called Ion cyclotron rather than Alfvén wave. In the  $\omega \ll \omega_{ci}$  limit, however, it behaves like an Alfvén

wave. The density in the middle of simulation domain was smoothly increased by a factor of 4 (a ramp-like function  $\rho(y) = 1 + 3 \exp[-((y-100)/50)^6]$ ) across the uniform magnetic field in order to model a coronal loop (accordingly temperature was varied as inverse of density so that total pressure balance is preserved). The widths of the transverse inhomogeneity on each side of the ramp is  $\approx c/\omega_{pi}$ . Fig. 5's left column demonstrates that initially plane Alfvén wave front becomes distorted (middle part travels slower) because its phase speed ( $V_A(y) = B_0/\sqrt{\mu_0\rho(y)}$ ) is a function of density, which in turn is a function of a coordinate  $y$  across the uniform magnetic field applied along  $x$ -axis. It is also interesting to note that in the strongest density gradient regions  $y = 50$  and  $150$  the propagating Alfvén wave damps. In the middle column of Fig. 5 parallel electric field  $E_{\parallel} = E_x$  is shown. At time  $t = 0$ ,  $E_{\parallel}$  is zero everywhere, but as the Alfvén wave propagates and its wave front becomes distorted  $E_{\parallel}$  starts to grow. It typically attains values of few  $10^{-3}(m_e c \omega_{pe}/e)$ . For solar coronal conditions this typically exceeds the Dreicer electric field (which is associated with the particle acceleration runaway regime (Dreicer 1959))  $10^6$  times! Hence, the generated parallel electric field efficiently accelerates electrons, as can be seen in the right column of Fig. 5. The latter shows parallel to the magnetic field phase space ( $V_x$  vs.  $x$ ) where each dot corresponds to an electron (total of  $\approx 5 \times 10^8$ ). We gather that in the regions where  $E_{\parallel}$  is generated, the num-

ber of particles with increased field-aligned velocity  $V_x$  is increased (i.e. particles are accelerated). Note that this coincides with the regions where Alfvén wave enhanced damping occurs. Tsiklauri & Haruki (2008b) performed a parametric study, exploring how the new mechanism of parallel electric field generation and acceleration of electrons discovered by Tsiklauri et al. (2005) depends on problem parameters, such as the variation of frequency and amplitude of the applied (driving) Alfvén wave, as well as plasma beta, affect levels attained by the  $E_{\parallel}$  and the fraction of accelerated particles (the latter is defined as percentage of electrons with speeds above the electron thermal speed in the density gradient regions). It was established that (i)  $E_{\parallel}$  is always orders of magnitudes greater than Dreicer electric field and (ii) the fraction of accelerated electrons ranges within 20-50%. The latter makes the discovered electron acceleration mechanism quite efficient and potentially capable of resolving the above mentioned problems of standard flare models which use reconnection-produced electron beams instead of waves as the means of delivering energy flux to the footpoints in order to produce the X-rays. It should be noted that the transverse inhomogeneity is crucial in the model of Tsiklauri et al. (2005) (see also further analysis paper (Tsiklauri 2007)). In fact, when the transverse density inhomogeneity is removed, i.e. when Alfvén wave front remains always perpendicular to the uniform background magnetic field, no parallel electric field generation or electron acceleration is observed (see Figs.7-10 in Tsiklauri et al. (2005)). In terms of the above  $k_{\perp}$  discussion, this can be explained as following: When the density across the magnetic field is inhomogeneous, despite the fact that initially  $k_{\perp} = 0$  as the Alfvén wave front starts to deform  $k_{\perp}$  is efficiently generated. When on the other hand density is constant everywhere then Alfvén wave front is always at right angles to the magnetic field, i.e. Alfvén wave propagates strictly along the field, and thus  $k_{\perp} = 0$  at all times. Recently, Fletcher & Hudson (2008) revisited the problem of solar flare electron acceleration with Alfvénic pulses. Further, McClements & Fletcher (2009) quantified the full details, namely, exploring how fraction of accelerated particles is affected by such crucial parameter as transverse length-scale  $l_{\perp} \simeq 2\pi/k_{\perp}$  of the Alfvénic pulse. They found that significant fraction of electrons would be accelerated if  $l_{\perp}$  is few meters or less. A clear distinction should be made between models of Tsiklauri et al. (2005) and McClements & Fletcher (2009). As explained above, in the case of former,  $k_{\perp}$  is *initially zero* and it seems that such wave is more plausible to exist in nature. This is because it represents simple, ubiquitous Alfvénic *harmonic* wave. Recall that even in MHD approximation  $k_{\perp}$  is also zero at all times. It is crucial in Tsiklauri et al. (2005)'s model that plasma has density inhomogeneity mimicking transverse density structure of the coronal loop. It is this inhomogeneity that makes Alfvén wave front to distort and create finite  $k_{\perp}$  and hence generate  $E_{\parallel}$ . In the case of McClements & Fletcher (2009)'s model  $k_{\perp} \neq 0$  (and hence  $E_{\parallel} \neq 0$ ) *from the start* and there is no transverse density inhomogeneity. Also, a pulse instead of harmonic wave is considered. If we try to compare plausibility of the two models the following considerations come to mind. Both models "work" i.e. generate large enough  $E_{\parallel}$  and accelerate sufficient proportion of electrons if the following are true: In Tsiklauri et al. (2005)'s model a large scale Alfvénic, har-

monic wave initially has  $k_{\perp} = 0$ , interacts with the transverse density inhomogeneity which has a scale of  $l_{inhom} \simeq c/\omega_{pi} \simeq c/\omega_{ci}$ . In McClements & Fletcher (2009)'s model (see their Eq.(28)) Alfvénic pulse with  $k_{\perp} \simeq 1/[A(c/\omega_{pi})]$  travels in the homogeneous plasma (where  $A$  is the perturbation amplitude). In effect, both models imply either small scale transverse inhomogeneity of the medium or small scale transverse wave number. It is unclear at this stage whether we have such small scale phenomena in solar corona. Perhaps, in situ coronal probes or remote sensing from distances much small than Sun-Earth distance could shed some light, as this is currently possible in Earth magnetospheric applications. However, until such times the jury on this topic will remain out.

In summary, wave based models offer attractive solutions to the above mentioned outstanding problems in solar flare particle acceleration. It is yet to be clarified however, how small-scale (kinetic-scale) phenomena feeds into the large-scale (MHD-scale) phenomena. From the fundamental point of view, of course kinetic-scale modelling includes all the essential physics. However, realistically shortcomings of man-made even the largest parallel supercomputers will unlikely offer us the performance we need. E.g. a full 3D Vlasov code 128 grids in the 6-dimensional phase space (3 spatial dimensions and 3 velocity dimensions) require 32 Terabytes (32,000 Gb) of RAM. Given that spatial grid size is the Debye length ( $\lambda_D = v_{th,e}/\omega_{pe} = 2.2 \times 10^{-3}$  m in the solar corona), in 3D this offers rather uninterestingly small physical volume. Thus, there is always a restriction imposed to consider a lower dimensional physical systems.

## 5 CHALLENGES AHEAD

Despite significant progress in understanding of physical processes ongoing in solar atmosphere – it is enough to take a look as NASA or ESA webpages describing a number of previous and existing successful space missions, as well future mission plans – there is still a long and exciting way to go! As far as coronal heating problem is concerned, in author's opinion further progress could be made if following considerations are noted.

From the observational perspective it would be rather important to investigate heating of active regions (ARs). AR is a volume of solar atmosphere above sunspots. They are important because during solar maximum ARs can be responsible for  $\approx 80\%$  of heating of the entire corona (Aschwanden et al. 2007). Top left of Fig.6 shows TRACE 171 Å image of an AR. The box in Fig.6 shows potential extrapolation (using Green's function method) of magnetic field lines based on an input from the measured normal component of the photospheric magnetic field that can be used for numerical modelling. Ideally, if we have *simultaneous*, high time cadence 2D imaging and 2D Doppler shift data at several wavelength,  $\lambda$ , corresponding to emission from e.g. white light (continuum, photosphere,  $\log(T) = 3.7$ ), HeII ( $\lambda = 304\text{Å}$ , chromosphere, transition region,  $\log(T) = 4.7$ ), FeIX ( $\lambda = 171\text{Å}$ , quiet corona, upper transition region,  $\log(T) = 5.8$ ) FeXII, FeXXIV ( $\lambda = 193\text{Å}$ , corona and hot flare plasma,  $\log(T) = 6.1, 7.3$ ), etc then one would be able to Fourier transform the data to see e.g. how much wave power spectrum is lost (dissipated) from one height (a hor-



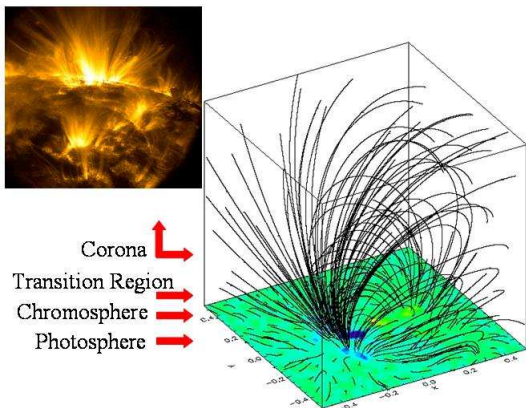


**Figure 6.** Top left panel shows TRACE 171 Å image of an active region in solar corona. The box shows potential extrapolation (using Green's function method) of magnetic field lines based on an input from the measured normal component of the photospheric magnetic field that can be used for numerical modelling.

horizontal cross-section through the box in Fig.6) to another. Essentially, different line forming ions probe different temperatures and therefore different heights in the box in Fig.6. This would ultimately enable us to make a judgement to what extent *waves* contribute to the AR and coronal heating? Also, measuring the abundance of the observed bi-polar jets, which are believed to be signatures of small-scale reconnection, could enable us to make a judgement on *reconnection's* contribution to the coronal heating. NASA's Atmospheric Imaging Assembly (AIA) on board of the Solar Dynamics Observatory (SDO), to be launched in November 2009, will make such unprecedented progress. However, AIA's resolution of about 1 arcsec and time cadence of 10 seconds or better will naturally limit the types of waves it can detect. Perhaps a better job could be done by a ground based project called Rapid Oscillations in Solar Atmosphere (ROSA), <http://star.pst.qub.ac.uk/rosa/>, which will have 0.1 arcsec resolution and will take in 30-125 frames per second! However, ROSA being a ground based instrument, can only probe photosphere/chromosphere/TR lines, i.e. cannot probe corona, and yet a whole wealth of new data is expected which will hopefully lead to new discoveries. On a negative note, with SDO's AIA and ROSA importance of kinetic effects still cannot be probed, because 1 arcsec on the Sun is  $0.72 \times 10^6$  m – orders of magnitudes larger than any kinetic scale discussed above. The concept of measuring wave dissipation with height has been used recently by Banerjee et al. (2009). This was based on variations in EUV line widths of coronal plumes (viewed off the solar limb) with height.

Also, there seems to be a serious gap in the studies of the coronal heating problem, as here are no studies which consistently would monitor global (*average*) coronal temperature. There are studies that monitor TSI (total solar irradiance) and its correlation to the (11 year-) solar activity cycle. Recent study by Frohlich (2009) suggests that the long-term trend of TSI is most probably caused by a global temperature change of the Sun (photosphere) that does not influence the UV irradiance in the same way as the surface magnetic fields. There is however, a work of Aschwanden & Acton (2001), where they split

the differential emission measure (DEM) into  $10^\circ$  sectors and estimate coronal heating requirement sector-by-sector. For every full-disk dataset with EUV and SXR coverage, it would be straightforward to compute a DEM of the entire corona, from which an emission measure-weighted temperature could be extracted as function of time. i.e. it could be possible to produce a graph of averaged (by all sectors i.e. full disk) coronal temperature as function of time, over the time interval of e.g.  $3 \times 11 = 33$  years with sufficient time cadence (e.g. once per year or more). Such plot would answer a significant question: whether the heat release in the corona is indeed related to the magnetic field (which we know changes on 11 year timescale). There is certainly a good correlation between the magnetic flux and SXR intensity (e.g. (Benevolenskaya et al. 2002), or see Fig. 1.13 in Aschwanden (2006) – Indeed, there seems to be a good case for  $I_{SXT}(t) \propto B^2$ ). However, it is questionable whether  $I_{SXT}(t)$  is a good proxy for global average coronal temperature, because SXR emission is non thermal (produced by the forbidden lines) – cf. Fig.2.3 from Aschwanden (2006) showing strong deviation of coronal emission from the blackbody spectrum. The analogy with a patient who has caught cold is relevant here: if a patient is sick, its temperature is routinely monitored by doctors. If we claim there is a coronal heating problem, indeed, solar physicists should monitor the global average temperature of their patient – the Sun's corona!

As far as modelling challenges are concerned, it seems a real progress can be made if two-fluid simulation of heating release in AR is attempted. When ion and electron dynamics is decoupled, we know that reconnection will proceed fast (Kuznetsova et al. 1998; Hesse et al. 1999; Birn et al. 2001; Pritchett 2001; Tsiklauri & Haruki 2007, 2008a) even without invoking anomalous resistivity. What is encouraging is that we do not need to use realistic ion to electron mass ratio of  $m_i/m_e = 1836$ . As previous results have shown, as long as ion-electron dynamics is decoupled simulation with  $m_i/m_e = 100$  is as good (Hesse et al. 2001; Tsiklauri & Haruki 2008a). This implies that significant reduction in CPU requirements can be achieved. The two-fluid simulation results then can be compared with the SDO's AIA and ROSA data to see whether inclusion of the two-fluid effects can provide fast enough reconnection or generated wave power and hence adequate coronal heating.

## ACKNOWLEDGMENTS

Author is supported by the Science and Technology Facilities Council (STFC) of the United Kingdom.

## REFERENCES

- Aschwanden M.J., Acton L.W., 2001, ApJ, 550, 475
- Aschwanden M.J., 2006, *Physics of the solar corona*, Springer and Praxis Publishing, Chicester
- Aschwanden M.J. et al., 2007, ApJ, 659, 1673
- Benevolenskaya E.E. et al. 2002, ApJ, 571, L181
- Banerjee D. et al., 2009, A&A, 501, L15
- Birkeland Kr., 1908, *The Norwegian aurora polaris expedition, 1902-1903*, London, New York, Longmans, Green & Co.

- Birn J. et al., 2001, *J. Geo. Res.*, 106, 3715  
Brown J.C., Melrose D.B., *Sol. Phys.*, 1977, 52, 117  
Campbell W. W., Moore J. H., 1919, *Lick Observ. Bulletin*, 10, 8  
Dalla S., Browning, 2008, *A&A*, 491, 289  
Daughton W. et al., 2006, *Phys. Plasm.*, 13, 072101  
De Moortel I. et al., 2008, *A&G*, 49, Issue 3, p. 3.21  
De Moortel I., 2009, *Sp. Sci. Rev.*, DOI 10.1007/s11214 – 009 – 9526 – 5  
Drake J.F., Shay M.A., 2007, In Ed. J. Birn, E.R. Priest, *Reconnection of Magnetic Fields*, p. 87, Cambridge U. Press, Cambridge  
Dreicer H., 1959, *Phys. Rev.* 115, 238  
Edwin P.M., Roberts B., 1983, *Sol. Phys.* 88, 179  
Edlén B., 1945, *MNRAS*, 105, 323  
Frankland E., Lockyer J.N., 1868, *Proc. R. Soc. Lond.*, 17, 288, DOI : 10.1098/r SPL.1868.0049  
Goldstein M.L., Roberts D.A., 1995, *ARA&A*, 33, 283  
Gudiksen B.V., Nordlund A., 2005, *ApJ*, 618, 1020  
Gudiksen B.V., 2009, *Adv. Sp. Res.* 43, 108  
Fletcher L., Hudson H.S., 2008, *ApJ*, 675, 1645  
Frohlich C., 2009, *A&A*, 501, L27  
Hasegawa A., Chen L., 1976, *Phys. Fluids* 19, 1924  
Hesse M. et al., 1999, *Phys. Plasm.*, 6, 1781  
Hesse M. et al., 2001, *J. Geophys. Res.*, 106, 3721  
Heyvaerts J., Priest E.R., 1983, *A&A*, 117, 220  
Horiuchi R., Sato T., 1997, *Phys. Plasm.*, 4, 277  
Ionson J.A., 1978, *ApJ*, 226, 650  
Kuznetsova M.M. et al., 1998, *J. Geo. Res.*, 103, 199  
Li B., Li X., Labrosse N., 2006, *J. Geo. Res.*, 111, A08106  
McClements K.G., Fletcher L., 2009, *ApJ*, 693, 1494  
Nakariakov V.M. et al., 1997, *Sol. Phys.*, 175, 93  
Nakariakov V.M., Ofman L., 2001, *A&A*, 372, L53  
Nakariakov V.M., Verwichte E., 2005, *Living Rev. Sol. Phys.*, 2, 3 <http://www.livingreviews.org/lrsp-2005-3>  
Pritchett P.L., 2001, *J. Geo. Res.*, 106, 3783  
Shay M.A. et al., 2007, *Phys. Rev. Lett.*, 99, 155002  
Siversky T.V., Zharkova V.V., 2009, *J. Plasma Phys.* (in press) eprint arXiv:0905.4687  
Stasiewicz K. et al., 2000, *Space Sci. Rev.* 92, 423  
Tsiklauri D. et al., 2001, *A&A*, 379, 1098  
Tsiklauri D., Nakariakov V.M., 2001, *A&A*, 379, 1106  
Tsiklauri D., Nakariakov V.M., 2002, *A&A*, 393, 321  
Tsiklauri D. et al., 2003, *A&A*; 400, 1051  
Tsiklauri D. et al., 2004, *A&A*, 419, 1149  
Tsiklauri D. et al., 2005, *A&A*, 435, 1105  
Tsiklauri D., 2007, *New J. Phys.*, 9, 262  
Tsiklauri D., Haruki T., 2007, *Phys. Plasm.*, 14, 112905  
Tsiklauri D., Haruki T., 2008a, *Phys. Plasm.*, 15, 102902  
Tsiklauri D., Haruki T., 2008b, *Phys. Plasm.*, 15, 112902  
Tsiklauri D., 2008, *Phys. Plasm.*, 15, 112903  
Yamada M. et al., 2006, *Phys. Plasm.*, 13, 052119  
Zharkova, V.V., Gordovskyy, M., 2005, *Space Sci. Rev.*, 121, 165